Region Specific Viscoelastic Properties of the Adult Rat Brain under Indentation following Traumatic Brain Injury

Lee F. Gabler, James R. Stone, Pierre D. Mourad, Jeff R. Crandall, Robert S. Salzar

Abstract Traumatic Brain Injury (TBI) is a serious health epidemic that places high societal and economic burdens on victims and their caregivers. Further, the associated neuropathological consequences that result from TBI are often complex and cause secondary injuries that are focal, diffuse and time dependent. Current computational models can predict loading and deformation associated with TBI; however, accurate knowledge of region specific material properties from both healthy and mechanically damaged brain is needed. In this study, the mechanical properties of both uninjured and traumatically injured brain tissue are presented. Adult male Sprague-Dawley rats were injured through a controlled cortical impact protocol. Ramp and hold indentation tests were performed at five locations on the surface of tissue samples excised from whole brain specimens. Force displacement data were analyzed using quasi-linear viscoelastic theory. An analysis revealed the tissue to be viscoelastic and spatially nonlinear with mechanical properties that depend on both region and level of injury. After normalizing the data, the nonlinear components of the instantaneous elastic force and shear modulus were found to be significantly lower, 26%, in the region containing the contusion cavity on severely injured samples compared to uninjured tissue at the same region in controls.

Keywords Traumatic brain injury, focal, diffuse, controlled cortical impact, mechanical damage, quasi-linear viscoelasticity

I. INTRODUCTION

Traumatic Brain Injury (TBI) is an important national health concern in the United States [1]. Approximately 1.7 million incidences and 52,000 deaths are reported annually due to automobile collisions, sports accidents, falls, and other head impacts [1]. Further, severe TBI has a high economic burden, costing nearly $76.5 billion each year in medical and societal costs [1]. On the battlefield, improvised explosive devices have led to TBI in as many as 62% of soldiers sustaining head injuries, and an estimated 360,000 service members have been affected by TBI over the past decade [2], [3]. Since the 1960s there has been a dramatic improvement in understanding the complex pathobiological behavior associated with TBI [4]. Brain injury, as a result of an impact or insult to the head, leads to a number of complex neuropathological consequences that result in further tissue dysfunction and eventually cell death [5]. However, injury quantification remains challenging because the neurochemical cascades that accompany TBI often involve complex secondary sequelae that are focal, diffuse, and time dependent [6]. A better understanding of the mechanical response of the brain during these events would improve diagnosis and treatment of TBI in both clinical and battlefield scenarios.

The material properties of brain during an injurious event were studied as early as the 1940s [7]. Not until more recently has an emphasis been placed on understanding the complex mechanical behavior of the brain during loadings that lead to TBI. Much of this can be attributed to an increase in awareness of the damaging, long-term effects following even mild brain injuries [1]-[3]. Material properties of brain are reported in the literature as viscoelastic [8]-[13], both spatially and temporally non-linear [9], [10], anisotropic [11], age-dependent [11]-[14], inhomogeneous [12], [13] and nearly incompressible [15]. Additionally, experimental factors such as specimen preparation, temperature [16] and level of hydration [14], [17] have been shown to influence these properties. There is considerable variation in the mechanical response reported in these

L.F. Gabler, B.A., J.R. Crandall, Ph.D., and R.S. Salzar, Ph.D., Department of Mechanical and Aerospace Engineering at the University of Virginia's Center for Applied Biomechanics, 4040 Lewis and Clark Drive, Charlottesville, VA 22911 USA (phone: (434) 296-7288 ext. 164, email: lfg4dc@virginia.edu). J.R. Stone, M.D., Ph.D., PI, Department of Radiology and Medical Imaging at the University of Virginia. P.D. Mourad, Ph.D., PI, Department of Neurological Surgery at the University of Washington.

studies. Much of this variation can be attributed to differences in the type of species, experimental protocols, and anatomical regions tested. Still, no definitive set of material properties exist for brain.

Computational models of TBI are commonly used to study the mechanical behavior of brain tissue during a traumatic event. Finite element modeling (FEM) can predict loading of various substructures through simulations of mild to severe TBI in rat brain [18]. These simulations have the added capability of predicting injury, because model-prediction of tissue strains were shown to correlate well with experimentally determined strain and strain rate injury tolerance criterion [19]-[21]. For more region-specific predictions of injuries, local material properties, including both traumatically injured and healthy brain tissue, need to be determined. Such knowledge would provide existing computational models with the added ability to predict the subsequent mechanical response of damaged tissue and allow for a better understanding of brain excitotoxicity beyond that of the initial trauma.

A survey of the literature revealed a number of studies that report thresholds for axonal damage. The reported mechanical limits for diffuse axonal Injury are between 0.1-0.2 Lagrangian strain at strain rates greater than $10s^{-1}$ [9], [19]-[22]. However, there is little information regarding changes in the mechanical properties of traumatically injured brain tissue. Shafieian et al. [23] used an impact acceleration model (IAM) to generate diffuse axonal injury (DAI) in the brainstem of adult male Sprague-Dawley (SD) rats. They reported a 35% reduction in the linear coefficient of the instantaneous shear modulus in injured rats compared to uninjured controls. Saxena et al. [24] studied traumatic spinal cord injury in adult female SD rats over the course of 2 and 8 weeks post injury. They observed a 50% reduction in elastic modulus for injured compared to healthy tissue. The goal of this study is to acquire accurate, region-specific material properties for both traumatically injured and uninjured rat brain to better understand the mechanical behavior of damaged tissue and to improve existing models of TBI.

II. METHODS

Animal Injury

All animal protocols were approved by the University of Virginia's Institutional Animal Care and Use Committee. Twenty adult male SD rats of average weight (mean ± SD), (320±27)gram, underwent surgical procedures for this study. Anesthesia was induced with a mixture of 4% isoflurane and 100% medical grade O_2 for 3-4 minutes in an induction chamber. Once the animals were sedated, the level of isoflurane was reduced to 2-2.5% and maintained for the duration of the surgery. The animals were then placed in a stereotaxic reference device (MyNeuroLab Leica Digital Stereotaxic Instrument, Leica Biosystems, Richmond, IL) and prepared for injury. A midline scalp incision was made along the forehead of each animal. The skin and underlying soft tissue were retracted exposing the sagittal, coronal, and lamboid sutures on the skull. A 4.5-5mm diameter hole was drilled from the skull above the right cerebral cortex exposing the dura at the coordinates of injury: *A* = -4mm bregma and *L* = 2mm (Ideal Micro-Drill™, Harvard Apparatus, Holliston, MA). An electromagnetically driven controlled cortical impact (CCI) device (MyNeuroLab Leica Impact One, Leica Biosystems, Richmond, IL) was used to deliver repeatable, severe, open head injury to nine of the animals; the remaining animals were prepared for *Sham* injury and used as controls. The 2mm diameter impact cylinder was positioned directly on the dura at the coordinates of injury. Contact between the probe tip and dura was verified via an electric circuit. The probe tip was then retracted from the dura and injury parameters were inputted to the device. Severe traumatic brain injury was delivered to the right ipsilateral cortex through a rapid 2.5mm compression of the dura, sustained for 200ms, with an initial impact velocity of 3.5m/s. In the instance of Sham injury, the impact probe was retracted from the dura, but no impact was performed on the tissue. The animals were then resuscitated and monitored for a period of twenty-four hours after which they were sacrificed and their brain tissue immediately collected.

Sample Preparation

Whole brain specimens were prepared for indentation tests immediately following tissue collection. To reduce the effects of temperature and level of hydration on the results, specimens were submerged in a physiological buffer (Millonig's Phosphate Buffer) for five minutes at room temperature (19-20)°C. Hydrated specimens were then placed into a coronal slice matrix (Braintree Scientific, Inc.) with incision planes spaced 1mm apart. Tissue cross-sections were cut to approximately 8mm in thickness from each whole brain specimen

using a 0.23mm thick razor blade (VWR Scientific, Media, PA). To accomplish this, two incisions were made in the coronal plane and parallel to each other. The first incision was made 1mm posteriorly to the injury plane at -5mm bregma and the second 8mm anteriorly to the first at 3mm bregma. In both Sham and severely injured specimens, the injury plane was identified by petechial hemorrhage on the dorsal surface of the tissue. However, in the case of a severe injury, the hemorrhage was more extensive and included a *contusion cavity*. Samples were then removed from the slicing matrix and placed on an aluminum test stage with the 5mm bregma coronal plane oriented upwards. The thickness of each sample deformed approximately 1mm under its own weight. The weight and dimensions of each sample were measured and recorded.

The coordinates of five regions, A-E, on the samples were determined using a stereotaxic reference frame [25] and are illustrated in Figure 1. Substructures of the brain under the indenter at these coordinates included both healthy and damaged tissue within the cerebral cortex, corpus callosum, hippocampus and midbrain. For severely injured samples, region A was located directly over the contusion cavity and within the injured hemisphere of the brain. Samples were assumed to be symmetric about the cerebral fissure, and regions B and D were located contralateral to regions A and C, respectively. Region E was positioned at approximately the center of the sample on the aqueduct. Coordinates were normalized to account for differences in the cross-sectional dimensions between samples due to intra-specimen variability. The normalization was performed by making length and width measurements on the cross-section of each sample; the five indentation coordinates were then multiplied by the ratio of the cross-sectional dimensions of the first sample tested under this protocol, ID NIB00287, to those of the sample of interest; the normalized coordinate locations were then dimensioned from region E using digital micrometers. Evan's Blue Dye was used to mark each coordinate on the tissue cross-section for a visual reference onto which the indenter could be positioned. The amount of dye under the indenter was assumed to have a negligible effect on the tissue properties. A total of 30 minutes were allotted for sample preparation, i.e. from the time of tissue collection to the time indentation testing began.

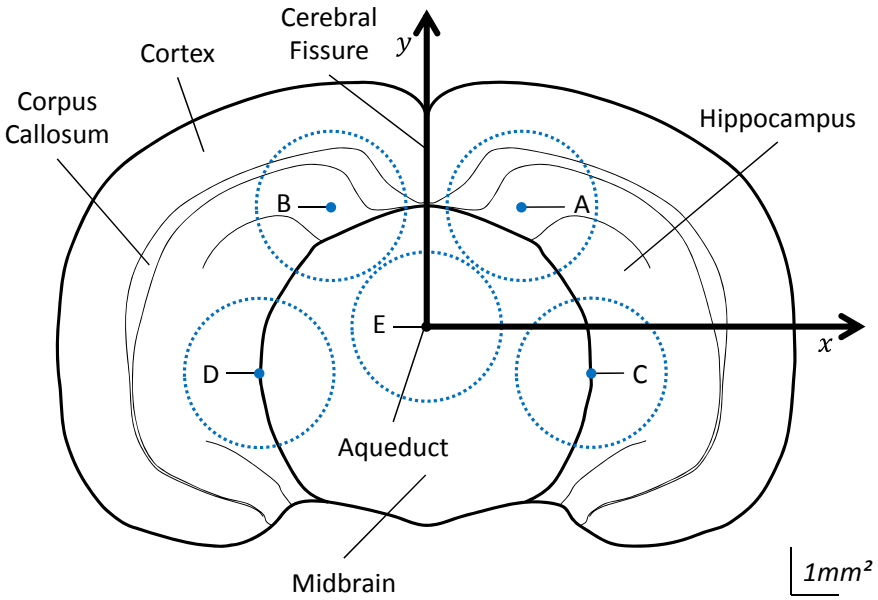

Figure 1: Schematic of a tissue sample showing the coordinate locations of the five un-normalized indentation regions (x, y): A = (2, 2.5), B = (-2, 2.5), C = (3.5, -1), D = (-3.5, -1) and E = (0, 0). Dashed circles represent the cross-sectional area of the indenter overlaid onto the tissue sample.

Indentation Testing

The aluminum test stage with sample was mounted atop a 50gram load cell (Model 31 Low, Honeywell International Inc., Golden Valley, MN), and beneath a 3.18mm diameter plane-ended cylindrical indenter mounted to a linear actuator equipped with an LVDT to measure displacement (ElectroForce® 3100 Test Instrument, Bose Corporation – ElectroForce Systems Group, Eden Prairie, MN). Excess compliance in the test frame due to the motion of the actuator induced an inertial based force response in the load cell. A 500g linear accelerometer (Model#: 7264B-500, Humanetics Innovative Solutions, Plymouth, MI) was mounted to the test stage to subtract off this effect. Force, displacement, and acceleration data were acquired at 20kHz (DEWE-

2010, Dewetron Inc., Wakefield, RI). Regions were tested in a randomized order for each experiment. At each coordinate the indenter was centered on the Evan's Blue Dye. This was accomplished by mounting a 1.3mm diameter spherical tip punch to the actuator and positing directly over the dye via visual inspection. The spherical punch was exchanged with the plane-ended cylindrical indenter, which was assumed to be centered over the indentation coordinate. The indenter was advanced slowly toward the tissue at a rate of 0.01mm/s until a tare load of 0.3gram was achieved. The indenter tip was then pressed 0.6mm into the tissue, normal with respect to the local surface, in approximately 8ms and then held for 30s to measure the tissue's relaxation. A peak displacement velocity of 120mm/s, at an approximate strain rate of $17s^{-1}$, was observed during the ramp portion of the displacement. After each test the indenter was carefully removed from the tissue. Five minutes were allotted between tests to allow for tissue recovery and instrumentation adjustments [26]. The tissue was sprayed with Millonig's in between each indentation test. The protocol was repeated for the remaining four regions and all testing was completed within 75 minutes of animal sacrifice.

Mathematical Modeling

All data were filtered in accordance to the SAE-J211 standard, CFC 1000, using a zero-phase, digital IIR 8 pole butterworth filter at a Low Pass frequency of 1650Hz. The data were resampled in a logarithmically scaled time step to give equal weights to both ramp and hold portions of the test. Samples were assumed to be incompressible and isotropic [9], [10]. The force response, $F(h,t)$, to the displacement input, $h = h(t)$, was modeled using a quasi-linear viscoelastic (QLV) mathematical framework [27]:

$$F(h,t) = \int_0^t G(t-t')\frac{\partial F^e(h)}{\partial h}\frac{\partial h}{\partial t'}dt' \tag{1}$$

where $F^e(h)$ is the instantaneous elastic response, $G(t)$ is the reduced relaxation function, t is the time, and t' is a dummy variable over which the convolution integral (1) is evaluated. The instantaneous elastic response was modeled using the solution to the Boussinesq problem for a flat-ended cylindrical punch [28]:

$$F^e(h) = \frac{4R\kappa\mu}{1-\nu}h \tag{2}$$

where R is the radius of the indenter, ν is Poisson's ratio, which was assumed to be 0.5, μ is the shear modulus, and κ is a constant used to incorporate the effect of substrate on finite sample thickness [29]. Values of κ were obtained for each sample and found to be between 1.26 and 1.3. The shear modulus was chosen to be a second-order, even function of h to capture the spatial nonlinearity of the tissue [23]:

$$\mu = \mu(h) = \mu_0 + \mu_2 h^2 \tag{3}$$

where μ_0 and μ_2 are the *instantaneous linear* and *nonlinear shear modulus coefficients*, respectively. Using this form for the shear modulus results in

$$F^e(h) = F_1 h + F_3 h^3 \tag{4}$$

where F_1 and F_3 are the *linear* and *nonlinear coefficients* of $F^e(h)$, respectively, described in (2). The mathematical solutions for the values of μ_0 and μ_2 in terms of F_1 and F_3 are determined through the use of equations (2-4).

$$\mu_0 = \frac{1-\nu}{4R\kappa}F_1 \qquad \mu_2 = \frac{1-\nu}{4R\kappa}F_3 \tag{5}$$

A six term prony series with five time constants was chosen to model the relaxation behavior of the tissue:

$$G(t) = G_\infty + \sum_{i=1}^{5} G_i \cdot e^{-\frac{t}{\tau_i}} \quad \text{under the constraint that} \quad G_\infty + \sum_{i=1}^{5} G_i = 1 \tag{6}$$

where G_i's are the normalized relaxation coefficients of the corresponding time decades and G_∞ is the coefficient of the steady-state response. Values for the thirteen coefficients F_1, F_3, τ_i, G_i, for i=1 to 5 and G_∞ were determined through a reduced gradient algorithm (Excel Solver®, Microsoft®, Redmond, WA) that was used to minimize the sum squared error between the model-predicted force, resulting from numerical integration of (1), and the experimental data. An individual set of optimal coefficients was determined for each indentation test. Preliminary analysis of the model fit to the first few data sets; test ID NIB00288A through NIB00288E, indicated marginal variability in the values for the optimized time constants, τ_1≈0.001s, τ_2≈0.01s, τ_3≈0.1s, τ_4≈1s, τ_5≈10s. To simplify the model the time constants were fixed at theses decades for the remainder of the analysis and only eight parameters needed to be optimized through model fitting.

Statistics

The number of terms, i, in equation (6) were determined via an F-test [30]. Data from test ID NIB00318E was modeled with four, five, and six time constants to see if there was a statistically significant improvement in the model's fit to the data. The model with five time constants gave a significantly better fit (F≈9, p < 0.001) than the model with four time constants and the model with six time constants showed no improvement in fit over five time constants (F≈0, p≈1). Therefore the model with five time constants was chosen for the analysis. The critical F-statistic at the α=0.05 level of significance for both tests was F_c ≈1. A total of n=8 indentation tests were performed per region, A-E, and per injury treatment, Sham and severe injury, for a total of 10 groups. For each group, an average $F^e(h)$ and $G(t)$ were determined using least squares optimization between the average and the eight individual measurements. The coefficients of the shear modulus, μ_0 and μ_2 were calculated from F_1 and F_3 of the eight individual curves using expression (5). An average μ_0 and μ_2 were then determined for each group. Additionally, the coefficients of $F^e(h)$ and $G(t)$ at regions A and C were normalized to the values at the contralateral regions B and D, respectively. Specifically, normalization was performed by dividing the value of a particular absolute coefficient F_1, F_3, μ_0 and μ_2 at region A by its corresponding absolute contralateral value at region B. For example, F_1 from indentation test ID NIB00290A was divided by F_1 from indentation test ID NIB00290B, etc. The process was repeated for the coefficients at region C, dividing by the corresponding contralateral values at region D. The absolute structural and material properties (F_1, F_3, μ_0, μ_2, G_i, for i=1..5 and G_∞) were compared separately to evaluate for the effect of region and injury treatment using a two-way ANOVA. *Post-hoc* comparisons were made using a student's t-test with the appropriate Bonferroni correction. Samples were assumed to be independent measurements of a particular tissue property, normally distributed and homoscedastic. To evaluate the differences observed in the normalized ratios, student's t-tests with a Bonferroni correction were used to make comparisons across injury treatment at a particular region. Specifically, a direct comparison was made between the normalized ratios of Sham and severely injured tissue at region A to evaluate the effect of injury at the location of the contusion cavity.

III. RESULTS

Eighty indentation tests were performed on the tissue samples, and data from 16 of the original 20 animals were used in analysis. The tissue from animal ID NIB00311 was damaged upon collection and the data from 3 additional experiments were compromised due to either unpreventable noise from the surroundings (animal ID NIB00287), or experimental error (animal IDs NIB00295 and NIB00298). Average $F^e(h)$ and $G(t)$ for region and injury treatment are shown in Figure 2. Region specific, *absolute* structural and material properties, *normalized* ratios, and results of the t-tests are reported in Table 1 (see appendix). ANOVA indicated significant (p < 0.05) main effects of both region and injury treatment on the absolute coefficients. On average, F_1 and μ_0 were higher (p < α=0.005) in region E compared to region A (F_1: +36.3mN/mm, p=0.002 and μ_0: +2.23kPa, p=0.002). The relaxation coefficient, G_1, was found to be higher while G_3 and G_∞ were lower (p < α=0.05) in severely injured samples compared to Sham controls (G_1: +0.011, p=0.0164, G_3: -0.003, p=0.008, and G_∞: -0.003, p=0.044). The student's t-test, revealed a significant decrease (p < α=0.025) in the value of the normalized ratios of F_3 and μ_2, (-26%, p=0.0084 each), in severely injured tissue compared to Sham controls. Conversely, the t-tests revealed a significant increase in the normalized ratios of F_3 and μ_2, (+38%, p=0.0156 each) on severely injured compared to sham controls in region C. The percentages reported here are calculated as percent differences in the sample means from Sham samples.

(Region A)

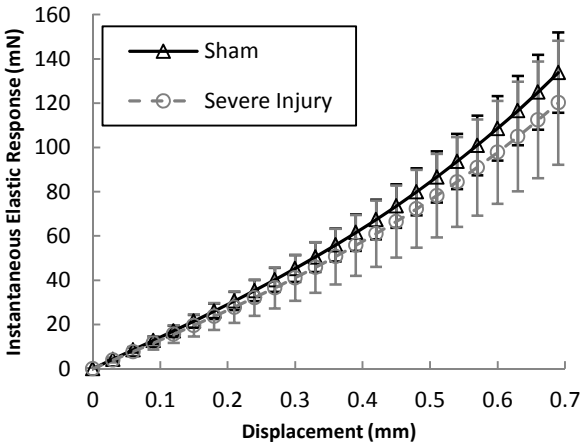

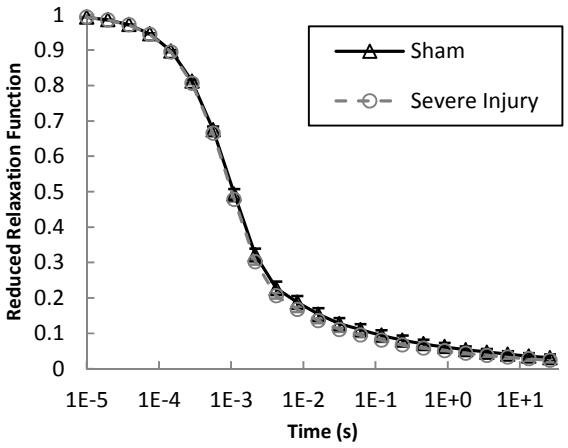

(Region B)

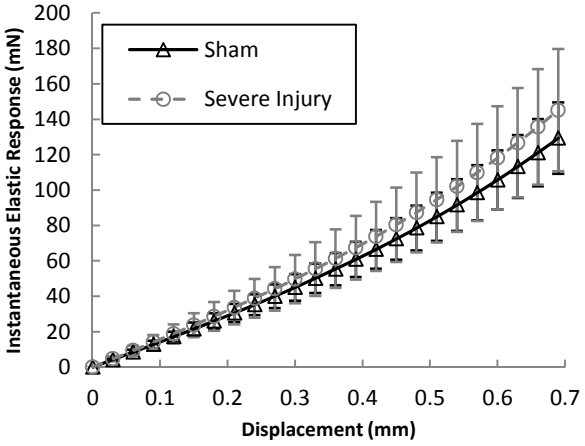

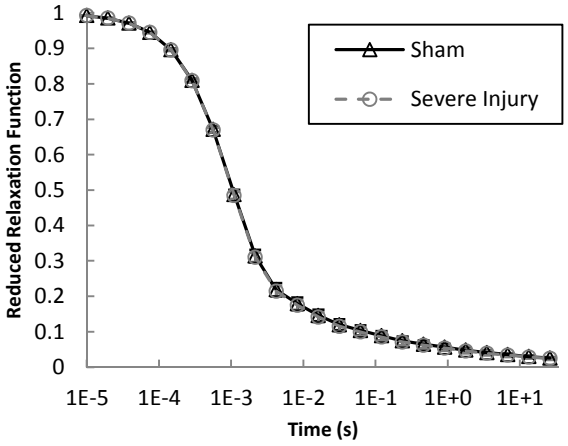

(Region C)

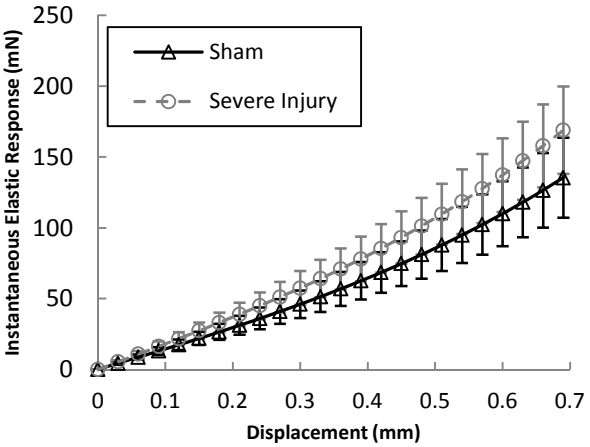

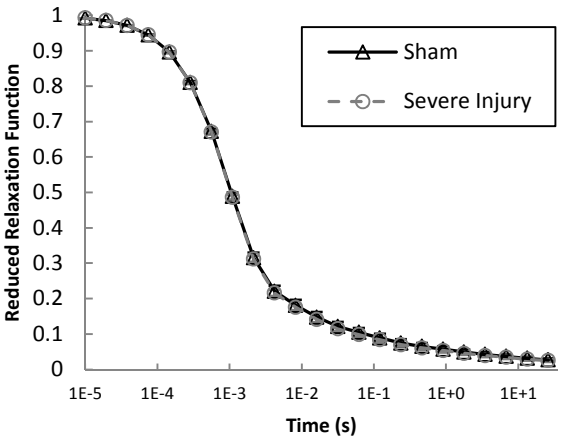

(Region D)

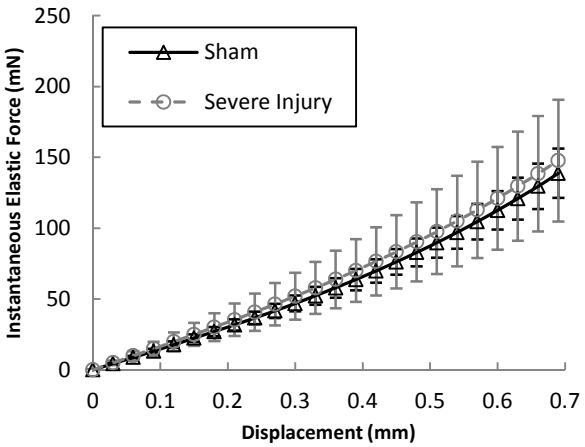

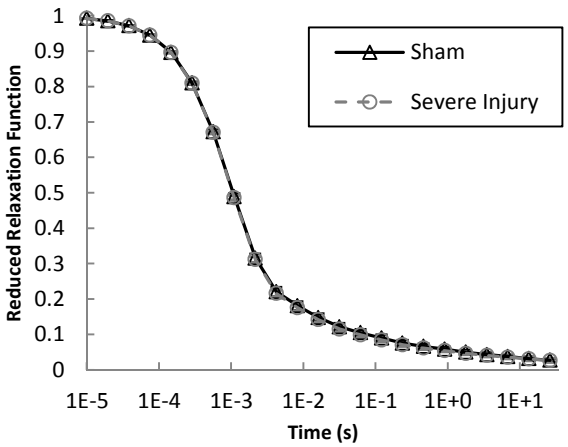

(Region E)

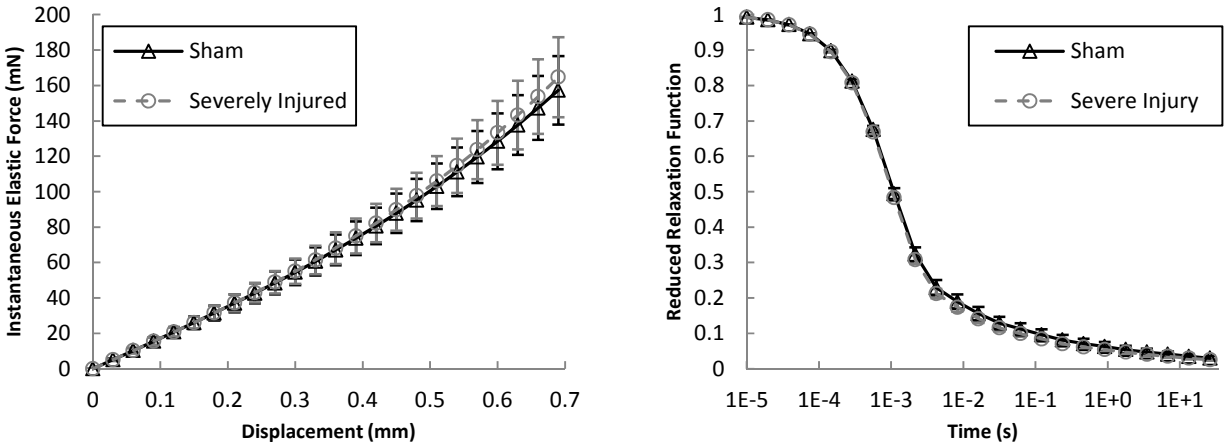

Figure 2: Average $F^e(h)$ and $G(t)$ for region and injury treatment. Error bars are 95% Confidence Intervals. Average $F^e(h)$ curves for severe injury were on average stiffer than the average Sham curves in all regions except for region A. The reduced relaxation functions were nearly identical in all cases.

IV. DISCUSSION

This study found the mechanical properties of the rat brain to be viscoelastic, spatially nonlinear, and dependent on both region and injury treatment. A linear viscoelastic model was fit to the experimental data, in addition to the QLV model, where equation (3) was assumed to be a function of μ_0 only. With the same number of prony series terms, the fits of both the linear and QLV models were visually assessed using tissue force time histories, and compared statistically using the F-test, Figure 3. The linear model fit the data well during the first of half of the ramp and long term relaxation of the tissue; however, the addition of the nonlinear term through QLV showed a statistically significant improvement in the model fit ($p < 0.001$) to the experimental data, capturing the entire ramp, peak force, and initial tissue relaxation, Figure 3a. To justify the use of QLV over a fully nonlinear viscoelastic model the ratio of the relaxation forces from two different displacement steps were calculated and then checked to be approximately constant in time using linear regression. Two displacement steps, the first to 0.6mm and the second to 1.2mm, were applied to tissue from a severely injured animal; ID NIB00291 at region A and region E. Results from the linear regression were used to evaluate whether or not the slope of the force ratio was statistically significant from zero. Data up to 100ms after the peak force were not included in the analysis due to transience of the displacement ramp. The value of the regression coefficient, the slope, was found to be statistically significant (slope = $0.035s^{-1}$, $p < 0.001$) at region A and (slope = $0.007s^{-1}$, $p < 0.001$) at region E. However, the magnitude of the slope was not thought to be meaningful. That is, the ability to detect small changes in the value of the slope was due to the large amount of data being used, and that the resulting values were not influential, suggesting a relatively constant response over time. These results indicated that the relaxation behavior of the tissue was independent of displacement and that no temporal nonlinearities were observed up to approximately 18% sample penetration.

(a) (b)

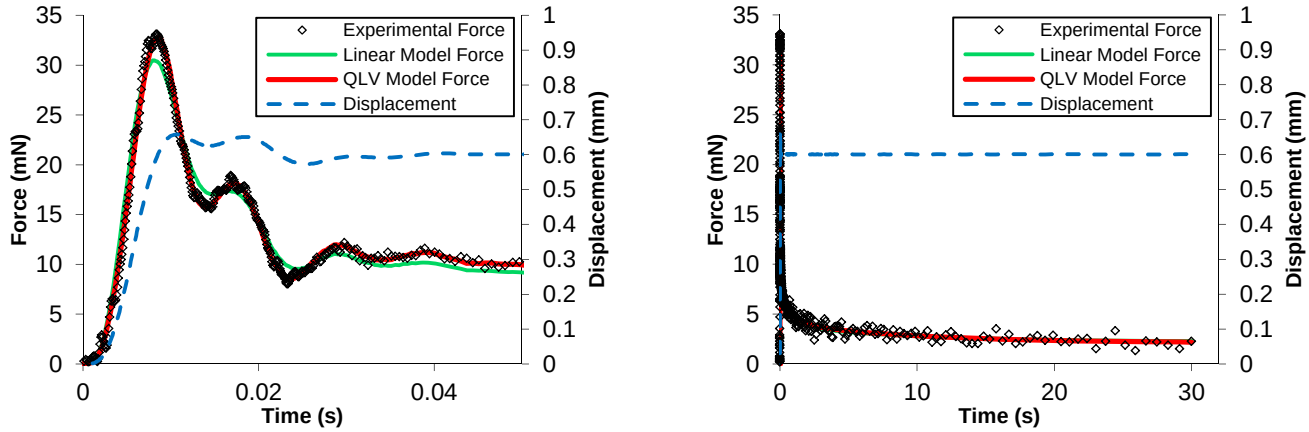

Figure 3: Examples of the QLV model fit to the experimental data for both the ramp (a) and hold (b) portions of an arbitrarily chosen indentation test (NIB00308B). The QLV model followed the experimental data more closely than the linear model during the ramp, peak, and initial relaxation of the tissue (a). Both models followed the data closely during the hold portion of the test (b). A similar result was observed when modeling other experimental data. The increase in force near 16ms and 30ms is due to the increase in displacement of the indenter into the tissue at these times.

Validation of the test methodology selected for the current study involves a comparison to other brain studies reported in the literature. The absolute mechanical properties and uncertainties found in the current study are consistent with those determined experimentally for shear [9], [31], compression [32] and indentation [23]. Further, the data fit within the reported range of shear moduli for brain tissue (0.1-22) kPa [8]-[16], [23] and [32]-[34]. Darvish and Crandall characterized bovine brain using QLV under oscillatory shear tests up to 200Hz and 20% Lagrangian strain [9]. They observed 16kPa and 2.62kPa for the linear and nonlinear instantaneous elastic shear moduli, respectively. On the other hand, Takhounts et al. tested both bovine and human brain up to 100% Lagrangian shear strain in ramp and hold tests and determined the instantaneous linear shear moduli to be approximately 2kPa and 1.5kPa, respectively [10]. Shuck and Advani found large variability in the shear modulus [31]. They performed oscillatory torsion tests on human brain up to 60Hz and observed (3-16)kPa. In each of these studies the brain was modeled under the assumptions of isotropy and incompressibility.

In regards to the results reported for indentation studies, Gefen et al. tested both young and mature rats in vivo and in situ under spherical indentation, and determined values for the instantaneous shear modulus between (1.2-3.3)kPa [15]. Further, Gefen and Margulies [33] compared the effects of in vitro, to in vivo and in situ on the material properties of porcine brain. They used a hemispherical indenter and found the short term shear modulus between (0.7-2.8)kPa. In both studies preconditioning was found to significantly reduce the value of the shear modulus and in vitro results tended to be lower than in vivo and in situ. Samples were not preconditioned in the current study as work by Shafieian et al. [23] suggests preconditioning may have damaged their samples and reduced the effect of injury. Various other studies have used micro-indentation to determine region specific material properties in rat brain [13], [34]. These studies observed values for the short term shear modulus on the order of (0.1-1.5)kPa, nearly one order of magnitude lower than the values reported in the current study. The material properties of brain have shown to be rate sensitive and increase with increasing strain rate or frequency [9] [10]. The load rates reported in these studies were less than 1mm/s, (0.4-0.5)s^{-1}, and much less than that of the current study which could explain this discrepancy. Additionally, these studies performed indentation tests up to depths of 40μm on the surface of tissue cross sections that had previously been blocked and then mechanically cut using a vibratome. Consequently, their findings may have been significantly altered from that of normal, healthy tissue. The tissue samples tested in the current study were hand cut and tested in vitro. As a result of sample preparation, a thin layer on the surface of the tissue likely sustained damage. Even though the indentation depths used in the current study were much higher than those used in micro-indentation, it is reasonable to expect some alterations in the mechanical properties from that of normal, healthy, living tissue.

In a similar study to the current, Shafieian et al. performed cylindrical indentation at two locations, PDx and PmJ, on the brainstem of impacted rats and found a statistically significant reduction in $F^e(h)$ between uninjured and injured specimens [23]. They reported values for μ_0 and μ_2 between (1-10)kPa and (1-25)kPa/mm^2, respectively with similar uncertainties to that of the current study. The reported reduction in μ_0 between injured specimens and Sham controls was 35%. This value was an average taken from both preconditioned and un-preconditioned samples and found to be in agreement with the work of Darvish and Crandall [12] who reported a 33% reduction in the linear shear modulus after non-recoverable strain conditioning. However, Shafieian et al. did not specify the significance of change in μ_0 and μ_2 with respect to injury treatment, making it unclear which parameter, if any, was driving the reduction in shear modulus after tissue damage [23]. On average, they saw a 28% and 47% reduction in μ_0 and μ_2, respectively, for un-preconditioned samples at PDx. Further, they observed a 14% and 29% reduction in μ_0 and μ_2 for un-preconditioned samples at PmJ; however, this result was not statistically significant. In the current study μ_0 and μ_2 were reduced on average 17% and 26%, respectively at the location of the contusion cavity, region A. This was observed after normalizing the data and the reduction in μ_0 was not statistically significant. In the case of

the absolute material properties, the observed differences in μ_0 and μ_2 between severely injured and Sham samples were not significant. Additionally, the reported 38% increase in μ_2 at region C on severely injured compared to sham tissue contradicts the findings for the normalized properties at region A. Further investigation into this matter is needed; however there was no evidence of mechanical damage in this region when compared to the visible damage of the contusion cavity in region A.

Possible reasons for these discrepancies can be attributed to a number of factors. In the current study, a CCI model was used to deliver injury directly to the cortex [35]. On the other hand, Shafieian et al. chose an impact acceleration model to generate DAI in the brainstem due to its predictable pattern of injury there [23], [36]. Further, regions tested in the current study incorporate both white and grey matter and are heterogeneous compared to the brainstem which is comprised of predominantly white matter and is relatively homogenous and stiffer than the cortex [37]. Another explanation for these discrepancies is the rate at which the tissue samples were loaded under indentation. Peak Loading rates determined from the tests conducted by Shafieian et al. [23] were between (16-33)mm/s, (8-16)s^{-1}, while that of the current study was approximately 120mm/s, 17s^{-1}. High rate inputs are necessary to characterize the mechanical response of the brain during TBI [38]. The peak loading rates reported in the current study are within the range of those reported for impact traumas [13], [38], and [39]. An understanding of the brain's mechanical response at high load rates would be useful for computational models of these events. However, testing at these rates may cause further damage to the tissue and reduce the effect of injury on the mechanical properties. Strain and strain rate tissue tolerance thresholds have previously been studied and the reported values associated with axonal injury are between 0.1-0.2 Lagrangian strain with strain rates greater than 10s^{-1} [9], [19]-[22].

The hypothesis that the tissue samples were damaged upon loading was examined in a separate analysis. A QLV model with only 1 time constant τ_1= 0.001s was fit to the ramp portion the experimental data (n=16) for region A. The form of $F^e(h)$ was kept the same as expression (4). The model was fit in three ways. The sum squared error was minimized between the model and experimental forces from: (1) the toe region to the force corresponding to the peak loading rate; (2) the force corresponding to the peak loading rate up to the peak force; and (3) over the entire ramp from the toe region to the peak force. Average $\mu_0$and μ_2 were determined from the (n=16) individual fits. ANOVA revealed significant ($p < 0.05$) differences between the three model fits. Post-hoc Bonferroni comparisons were made between individual samples and revealed the following information. The value of μ_0 was approximately constant across all three models, while the value of μ_2 decreased by 34% ($p < 0.001$) after the peak displacement rate of 120mm/s. This observation was made independent of injury treatment. The stability of the model was evaluated during each of the three fits due to the relatively small amount of data being fitted. Regardless of initial inputs, model parameters optimized to the same values, indicating a stable solution. These results suggest that the tissue may have been damaged during loading up to 5% tissue penetration and at a peak rate of 17s^{-1}.

V. CONCLUSIONS

This study presents an experimental methodology and analytical framework for modeling the region specific structural and material properties of mechanically injured and uninjured brain tissue. Force data were acquired under high rate loading inputs in the range of those related to impact traumas. Quasi-linear viscoelasticity, a popular, constitutive model that is commonly used to model soft biological materials was chosen to fit the experimental data over both linear and fully nonlinear viscoelastic models. The tissue was assumed to be isotropic and incompressible for model simplification. The mechanical properties were found to be viscoelastic, nonlinear, and regionally dependent. Additionally, these properties were quantified under a well characterized injury model capable of delivering repeatable levels of mechanical damage directly to the dura. To the authors' knowledge, this is the first study to examine the mechanical properties of the brain after CCI. The results for the shear modulus were within the range reported in the literature for shear, compression, and indentation tests. The material and structural properties were found to be roughly constant across region and injury treatment. However, after normalizing the region specific mechanical properties in regions A and C, there were statistically significant differences in the values of the nonlinear coefficients of the instantaneous shear and elastic response. A 26% reduction in the nonlinear material and structural coefficients were observed in severely injured samples compared to healthy controls at the location of the contusion cavity. The utility of this research is crucial for understanding the mechanical response of the brain after TBI. Knowledge of such

material properties may be useful to uniquely identify different types of brain injury and to better understand the mechanics of repetitive brain injuries.

VI. LIMITATIONS

There are a number of limitations that may influence overall response of the tissue samples during mechanical loading. First, the solution to the Boussinesq problem assumes indentation of a semi-infinite elastic half-space. The samples used in the current study have finite boundaries and exhibit damping as well as elastic properties. This solution was modified by [29] to incorporate the effect of a rigid substrate on finite sample thickness. The corrective factor κ was developed for indentation on articular cartilage and subsequently applied to indentation tests performed on other soft biological tissues including brain [13], [23]. The factor κ functions to reduce the applied load, measured within the tissue, by an amount that depends on the ratio of the indenter radius to sample height. As the indenter radius increases or sample height decreases, higher forces are transmitted from the substrate to the tissue. To avoid the effect of substrate on mechanical properties, a common rule of thumb is to limit indenter penetration to depths of no greater than 10% of the total sample thickness [40]. Penetration depths in the current study obey this rule. However, more recent work has observed noticeable substrate effects within 10% penetration and claim that the ratio of the indenter radius to sample height must be kept within 10% [41]. The ratio of radius to sample height is 20% in the current study and κ was implemented to adjust for this limitation. In addition to substrate effects, other boundary conditions have been violated. In all regions except E, the distance between the indenter and edge of the tissue sample was less than the recommended distance of one indenter's width. This would have the effect of reducing the material properties observed in regions A-D compared to E. Indenter interference is an additional concern in this study. The process by which the coordinates were dimensioned on the surface of the tissue was imperfect. Slight offsets in the dimensioning may have led to overlapping indentation tests. Further, the indentations made on the surface of the samples were within one diameter of each other. However, adequate time was allotted for tissue recovery in between subsequent tests. Finally, contusion cavities can be problematic for material studies [23]. They are often near the edge of the sample and create discontinuities in the tissue surface making it difficult to obey boundary conditions under most mechanical tests. It is suggested that future studies involving contusion cavities be made in vivo or situ with the brain left in the skull.

A number of studies including the current have used the F-test to statistically determine an appropriate model for fitting experimental brain data [13], [23], [34]; however, there are limitations. The F-test assumes the data to be independently measured and normally distributed. In addition, there must be a linear relationship between independent and dependent variables in the models chosen to fit the data. The force data in the current study are not normally distributed and not independent measurements in time. Further, in both the linear viscoelastic and QLV models the relationship between force and time is not linear. Therefore it is not clear that hypothesis testing using the F-test is suitable or meaningful to determine the most appropriate model. In this case, visual inspection of the model fit to the data may provide a better indicator of goodness of fit.

VII. ACKNOWLEDGEMENT

This work was performed at the University of Virginia, and in collaboration with the University of Washington. Funded in part by the Defense Medical Research and Development Program (DMRDP), award No. DM090796.

VIII. REFERENCES

[1] Faul M, Xu L, Wald MM, Coronado VG, "Traumatic brain injury in the United States: emergency department visits, hospitalizations, and deaths, Atlanta (GA): Centers for Disease Control and Prevention, National Center for Injury Prevention and Control, 2010", Internet: [http://www.cdc.gov/traumaticbraininjury/tbi_ed.html], January 7, 2013, [February 21, 2013]

[2] Owens BD, Kragh JF Jr, Wenke JC, Macaitis J, Wade CE, Holcomb JB, Combat wounds in Operation Iraqi Freedom and Operation Enduring Freedom, *Journal of Trauma-Injury Infection & Critical Care*, 64(2):295-299, 2008.

[3] Pascrell B Jr, Congressman, Introduction to the report of the international conference on behavioral health and traumatic brain injury, *The Clinical Neuropsychologist*, 23(8):1281-1290, 2009.

[4] Farkas O, Povlishock JT, Cellular and subcellular change evoked by diffuse traumatic brain injury: a complex web of change extending far beyond focal damage, *Progress in Brain Research* 161:43-58, 2007.
[5] McAllister TW, Neurobiological consequences of traumatic brain injury*, Dialogues in Clinical Neuroscience*, 13(3):287-300, 2011.
[6] Povlishock JT, Katz DI, Update of neuropathology and neurological recovery after traumatic brain injury, *The Journal of Head Trauma Rehabilitation* 20(1):76-94, 2005.
[7] Holbourn AHS, Mechanics of head injury, *The Lancet*, 2, 6267, 438-441, 1943.
[8] Galford JE, McElhaney JH, A viscoelastic study of scalp, brain, and dura, *Journal of Biomechanics*, 3(2):211-221, 1970.
[9] Darvish K, Crandall JR, Nonlinear viscoelastic effects in oscillatory shear deformation of brain tissue, *Medical Engineering & Physics*, 23:633-645, 2001.
[10] Takhounts EG, Crandall JR, Darvish KK, On the importance of nonlinearity of brain tissue under large deformations, *Stapp Car Crash Journal*, 47:79-92, 2003.
[11] Gefen A et al., Age-dependent changes in the material properties of the brain and braincase of the rat, *Journal of Neurotrauma*, 20(11):1163-1177, 2003.
[12] Prange MT, Margulies SS, Regional, directional, and age-dependent properties of the brain undergoing large deformation, *Journal of Biomechanical Engineering*, 124:244-252, 2002.
[13] Finan JD, Pearson EM, Morrison III B, Viscoelastic properties of the rat brain in the horizontal plane, *Proceedings of IRCOBI Conference*, Dublin, Ireland, pp. 474-485, 2012.
[14] Thibault KL, Margulies SS, Age-dependent material properties of the porcine cerebrum: effect on pediatric inertial head injury criteria, *Journal of Biomechanics* 31(12):1119-1126, 1998.
[15] McElhaney JH, Roberts VL, Hilyard JF, Handbook of Human Tolerance, Japan Automobile Research Institute, Incorporated (JARI), p. 143, 1976.
[16] Arbogast KB et al., A high-frequency shear device for testing soft biological tissues, *Journal of Biomechanics,* 30(7):757-759, 1997.
[17] Dobbing J, The later development of the brain and its vulnerability. In: Davis J A, Dobbing J (Eds.), Scientific Foundations of Paediatrics, *Heinemann Medical*, London, UK, 1974.
[18] Mao H, Jin X, Zhang L, Yang KH, Igarashi T, Noble-Haeusslein LJ, et al., Finite element analysis of controlled cortical impact-induced cell loss, *Journal of Neurotrauma*, 27(5):877-88, 2010.
[19] Elkin BS, Morrison B III, Region-specific tolerance criteria for the living brain, *Stapp Car Crash Journal,* 51: 127-138, 2007.
[20] Cater HL, Sundstrom LE, and Morrison B, Temporal development of hippocampal cell death is dependent on tissue strain but not strain rate, *Journal of Biomechanics* 39(15):2810-2818, 2006.
[21] Morrison III B, Cater HL, Wang CC, Thomas FC, Hung CT, Ateshian GA, et al., A tissue level tolerance criterion for living brain developed with an in vitro model of traumatic mechanical loading, *Stapp Car Crash Journal*, 47:93-105, 2003.
[22] Bain AC, Meaney DF, Tissue-level thresholds for axonal damage in an experimental model of central nervous system white matter injury, *Journal of Biomechanical Engineering,* 122:615-622, 2000.
[23] Shafieian M, Darvish KK, and Stone JR, Changes to the viscoelastic properties of brain tissue after traumatic axonal injury, *Journal of Biomechanics,* 42(13):2136-2142, 2009.
[24] Saxena T, et al., Mechanical characterization of the injured spinal cord after lateral spinal hemisection injury in the rat, *Journal of Neurotrauma*, 29(9):1747-1757, 2012.
[25] Paxinos G, Watson C, The Rat Brain in Stereotaxic Coordinates 5th Edition, Bregma -5.04 mm, *Elsevier*, Oxford, UK, 2005.
[26] Hrapko M et al., The mechanical behavior of the brain tissue: Large strain response and constitutive modeling, Biorheology, 43:623-636, 2006.
[27] Fung YC, Biomechanics: Mechanical Properties of Living Tissues, 277-280, *Springer*, New York, NY, 1993.
[28] Sneddon IN, The relation between load and penetration in the axisymmetric Boussinesq problem for a punch of arbitrary profile, *International Journal of Engineering Science* 3(1):47-57, 1965.
[29] Hayes WC, Keer LM, Herrmann G, and Mockros LF, A mathematical analysis for indentation tests of articular cartilage, *Journal of Biomechanics*, 5(5):541-551, 1972.

[30]Motulsky HJ, Cristopoulos A, Fitting Models to Biological Data using Linear and Nonlinear Regression. A Practical Guide to Curve Fitting. 2003, GraphPad Software Inc., San Diego CA, www.graphpad.com.
[31]Shuck LZ, and Advani SH, Rheological response of human brain tissue in shear, *Journal of Basic Engineering*, 94 (D), 905-911, 1972.
[32]Estes MS and McElhaney JH, Response of the brain tissue of compressive loading. ASME, No 70-BHF-13, 1970.
[33]Gefen A, Margulies SS, Are in vivo and in situ brain tissues mechanically similar? *Journal of Biomechanics*, 37:1339-1352, 2004.
[34]Elkin BS, Ilankovan A, and Morrison III B, A detailed viscoelastic characterization of the rat brain*, Journal of Neurotrauma* 28:2235-2244, 2011.
[35]Lighthall JW, Controlled cortical impact: a new experimental brain injury model, *Journal of Neurotruama*, 5(1):1-15, 1988.
[36]Marmarou A et al., A new model of diffuse brain injury in rats, *Journal of Neurosurgery* 80:291-300, 1994.
[37]Arbogast K, Margulies S, Material characterization of the brainstem from oscillatory shear tests, *Journal of Biomechanics* 31(9):801–807, 1998.
[38]Mertz HJ, Anthropomorphic test devices, In: Nahum, A.M., Melvin, J.W. (Eds.), Accidental Injuries. *Springer,* New York, pp. 72–88, 2002.
[39]Hardy WN et al., A study of the response of the human cadaver head to impact, *Stapp Car Crash Journal* 51:17, 2007.
[40]Bückle H, Progress in micro-indentation hardness testing, *Metallurgical Reviews*, 4(1):49-100, 1959.
[41]Wang M et al., Nanoindentation of polymeric thin films with an interfacial force microscope, *Journal of the Mechanics and Physics of Solids*, 52:2329-2354, 2004.

IX. APPENDIX

Table 1: Absolute Structural and Material Coefficients of $F^e(h)$, $G(t)$, and $\mu(h)$ and Normalized Ratios for Region and Injury Treatment.

Absolute		A				B				C			
Unit	Coef.	Sham		Severe Injury		Sham		Severe Injury		Sham		Severe Injury	
mN/mm	F_1	140.8 ± 19.2		128.2 ± 33.0		141.1 ± 24.1		155.2 ± 44.7		143.4 ± 30.7		179.0 ± 38.7	
mN/mm³	F_3	111.6 ± 24.1		96.6 ± 19.7		97.3 ± 17.4		115.6 ± 22.3		110.8 ± 23.6		138.1 ± 16.4	
kPa	μ_o	8.66 ± 1.23		7.89 ± 2.04		8.68 ± 1.51		9.55 ± 2.76		8.85 ± 2.00		11.02 ± 2.40	
kPa/mm²	μ_2	6.88 ± 1.57		5.95 ± 1.23		5.99 ± 1.12		7.11 ± 1.38		6.83 ± 1.53		8.50 ± 1.03	
-	G_1	0.739 ± 0.021		0.763 ± 0.010		0.749 ± 0.021		0.752 ± 0.015		0.746 ± 0.018		0.750 ± 0.010	
-	G_2	0.122 ± 0.007		0.117 ± 0.007		0.121 ± 0.006		0.123 ± 0.004		0.122 ± 0.006		0.126 ± 0.004	
-	G_3	0.057 ± 0.005		0.053 ± 0.004		0.055 ± 0.002		0.053 ± 0.006		0.057 ± 0.003		0.054 ± 0.003	
-	G_4	0.029 ± 0.005		0.026 ± 0.002		0.029 ± 0.008		0.028 ± 0.003		0.027 ± 0.005		0.027 ± 0.002	
-	G_5	0.023 ± 0.007		0.020 ± 0.005		0.023 ± 0.008		0.022 ± 0.006		0.023 ± 0.004		0.021 ± 0.002	
-	G_∞	0.029 ± 0.009		0.022 ± 0.005		0.024 ± 0.003		0.022 ± 0.003		0.025 ± 0.004		0.023 ± 0.004	

Absolute		D				E			
Unit	Coef.	Sham		Severe Injury		Sham		Severe Injury	
mN/mm	F_1	145.7 ± 18.4		163.6 ± 54.1		170.8 ± 24.0		170.7 ± 21.8	
mN/mm³	F_3	116.2 ± 33.5		106.0 ± 20.6		120.2 ± 32.3		142.8 ± 24.5	
kPa	μ_o	8.96 ± 1.15		10.07 ± 3.35		10.49 ± 1.42		10.51 ± 1.39	
kPa/mm²	μ_2	7.17 ± 2.15		6.52 ± 1.28		7.42 ± 2.07		8.79 ± 1.54	
-	G_1	0.746 ± 0.015		0.750 ± 0.009		0.737 ± 0.024		0.756 ± 0.015	
-	G_2	0.122 ± 0.006		0.125 ± 0.003		0.122 ± 0.007		0.118 ± 0.004	
-	G_3	0.055 ± 0.004		0.054 ± 0.003		0.059 ± 0.004		0.056 ± 0.004	
-	G_4	0.028 ± 0.004		0.026 ± 0.002		0.029 ± 0.005		0.024 ± 0.004	
-	G_5	0.024 ± 0.007		0.020 ± 0.004		0.025 ± 0.010		0.023 ± 0.005	
-	G_∞	0.025 ± 0.005		0.025 ± 0.006		0.028 ± 0.006		0.024 ± 0.002	

Normalized Ratios		A					C				
Unit	Coef.	Sham			Severe Injury		Sham			Severe Injury	
-	F_1	1.017 ± 0.144			0.843 ± 0.145		0.999 ± 0.228			1.187 ± 0.357	
-	F_3	1.149 ± 0.182	*		0.848 ± 0.144		0.992 ± 0.158	†		1.361 ± 0.275	
-	μ_o	1.017 ± 0.144			0.843 ± 0.145		0.999 ± 0.228			1.188 ± 0.357	
-	μ_2	1.149 ± 0.182	**		0.848 ± 0.144		0.992 ± 0.158	††		1.362 ± 0.276	

All symbols indicate a statistically significant result. Asterisks (*,**) and daggers (†,††) are comparisons between injury treatment at a particular region. (p = resulting p-value from a student's t-test and α = 0.025 is the Bonferroni corrected significance level). (*p = 0.0084, **p = 0.0085, †p = 0.0156, ††p = 0.0156. All uncertainties are ±95%CI.